This article has been accepted for publication in IEEE Microwave and Wireless Technology Letters. This is the author's version which has not been fully edited and content may change prior to final publication. Citation information: DOI 10.1109/LMWT.2024.3474971

Microwave Radiometer Calibration using Low-Noise Amplifier as Calibration Source

Reuben Neate and Tinus Stander, *SMIEEE*

***Abstract*—We present a novel method for built-in noise and gain calibration of a total power radiometer using a low-noise amplifier (LNA) as the calibration source. A terminated LNA's biasing is varied to obtain multiple calibration points, with the novel post-processsing method accounting for both radiometer nonlinearity and unknown LNA parameters. This method allows for a built-in radiometer calibration without a calibrated resistive or diode noise source, instead using an internal thermometer measurement as reference. The method is demonstrated by measuring a thermal load to a 24 GHz water vapour radiometer, achieving a mean error of 0.43 K over the band of interest under 45°C ambient temperature variation. It is further shown that the calibration data can be used to estimate the radiometer's gain to within 1.41 dB, and noise figure to within 0.55 dB.**

***Index Terms*—Atmospheric monitoring, noise calibration, remote sensing, water vapour radiometer, Y-factor**

I. Introduction

A microwave water vapour radiometer (WVR) determines atmospheric water vapour content by using an RF receiver to relate a power detector voltage measurement (V_{out}) to a sky brightness temperature (T_{in}) by the simplified linear expression

$$V_{out} = a \times T_{in} + b \tag{1}$$

where a and b represent the linear fitting coefficients. These are subject to variation over time, and requires in-situ calibration [1], [2]. Many common calibration methods involve viewing an external black body of known brightness temperature, or atmospheric observation with tip-curve calibration, both of which require a physical moving antenna or human interaction [2], [3]. Failure of the moving parts required for tip curve calibration, in particular, is a major challenge to long-term remote site surveying [4]–[6]. Alternatively, many WVRs are equipped with internal noise sources, such as a noise diode, arranged in a switching configuration [2], [7]. These, however, require accurate prior calibration data, increasing the cost significantly. Alternatively, an active device, such as a low-noise amplifier (LNA) terminated with a matched load, can be used as an internal noise source, with noise temperature (T_N) described by [8], [9]

$$T_N = T_{ref} \times 10^{\frac{NF+G}{10}} + T_p \tag{2}$$

where T_{ref} is the reference temperature for the LNA's noise figure (NF) (usually 290 K), G and NF are the amplifier's average gain and noise figure over the band (both in dB), and T_P is the terminating load's physical temperature [10]. If G and NF of the noise source LNA are exactly known, (2) can be used to determine the T_N. Using (1) and two calibration points, a radiometer can be calibrated. However, both G and NF vary with temperature and production tolerance.

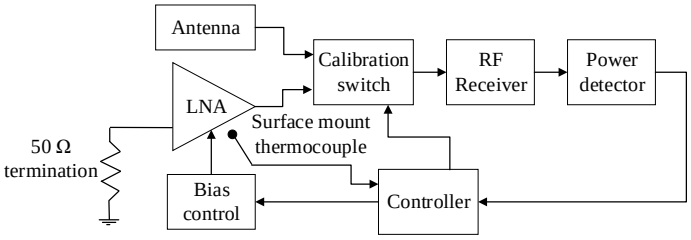

Fig. 1: Block diagram of radiometer configuration.

This paper proposes a novel method to calibrate a K-band WVR using a poorly characterised LNA as a noise source, aided by a secondary post-processing step to enhance calibration accuracy using an internal thermometer measurement as reference. It extends on the methods proposed by [8], [9], by introducing a step to account for uncertainty in LNA G and NF to increase calibration accuracy. The proposed method eliminates the need for tip curve calibration and the associated moving parts, calibrated noise sources and external calibration targets, enabling K-band WVRs for remote site surveying [11] using low-cost off-the-shelf components without moving parts or temperature control.

II. Approach

The system topology (Figure 1) shows the RF receiver connected to a power detector at the output and a calibration switch at the input, switching either the antenna or a calibration noise source to the receiver. For the noise source, an off-the-shelf LNA is used, with its output connected to the calibration switch and its input terminated in a 50 Ω load. A surface mount thermocouple is co-located on the PCB, to monitor the physical LNA temperature, T_P. The thermal noise from the LNA (T_{PLNA}) when turned off (zero bias voltage V_{B0}) can be estimated as $T_{PLNA} = dT_P$, where d is the noise power transfer coefficient due to loss and impedance mismatch [12].

The calibration procedure follows the post-processing algorithm shown in Algorithm 1:

1) Set the calibration switch to the antenna input and record the radiometer output (V_{ANT}).
2) Set the calibration switch to the noise source LNA and record n noise source voltage measurements ($V_{N1...n}$) with different noise source bias voltages ($V_{B1...n}$).
3) Turn the noise source LNA off and record the V_{N0} for $V_{B0} = 0V$ and the physical LNA temperature, T_P.
4) Generate an initial estimate for noise temperature output of the LNA ($T_{N1...n}$), for $V_{B1...n}$, based on datasheet

This article has been accepted for publication in IEEE Microwave and Wireless Technology Letters. This is the author's version which has not been fully edited and content may change prior to final publication. Citation information: DOI 10.1109/LMWT.2024.3474971

Algorithm 1 Post-processing algorithm

Input: An array T_N of n elements, an array V_N of n elements, V_{ANT}, V_{N0}, T_{PLNA}, $c = 0.1$, $tol = 0.01$
Output: T_{ANT} as the antenna brightness temperature
$m \leftarrow 1$
for $i = 1$ to $n - 1$ **do**
  for $j = i + 1$ to n **do**
    $E = tol + 1$
    while $|E| > tol$ **do**
      $a \leftarrow \frac{V_N[j]-V_N[i]}{T_N[j]-T_N[i]}$
      $b \leftarrow V_N[j] - aT_N[j]$
      $E \leftarrow T_{PLNA} - (\frac{V_{N0}-b}{a})$
      if $|E| > tol$ **then**
        $T_N[i] \leftarrow T_N[i] - cE$
        $T_N[j] \leftarrow T_N[j] + cE$
      end if
    end while
    $T_{ANT} \leftarrow T_{ANT} + \frac{V_{ANT}-b}{a}$
    $m \leftarrow m + 1$
  end for
end for
$T_{ANT} \leftarrow \frac{T_{ANT}}{m}$
Return: T_{ANT}

estimates and (2), though faster convergence might be obtained from prior VNA and Y-factor measurements of the LNA.

5) For ($T_{N1...n}$), fit a straight line through [T_{Ni};V_{Ni}] and [T_{Nj};V_{Nj}] in the form of (1). i and j can be any two points from 1 to n as long as $i < j$.
6) Test if the fitted line from step 5 passes through the point [T_{PLNA};V_{N0}]. If not, return to step 5 with $T_{Ni} = T_{Ni} - cE$ and $T_{Nj} = T_{Nj} + cE$. E is the error between T_{PLNA} and the position for T_{PLNA} predicted by fitted line and V_{N0}. c is a constant and should be chosen $c << 1$, with a reasonable choice being $c\epsilon$[0.01,0.1].
7) Calculate the antenna brightness temperature ($T_{ANT,1...m}$) from V_{ANT} and (1). $m = \binom{n}{2}$ to represent every combination of i and j.
8) Average the results for $T_{ANT,1...m}$ for a final T_{ANT}.

The averaged T_{ANT} value is the best estimate of the true radiometric scene temperature, with larger samples providing more accurate results.

While it is common practice (for a well-calibrated noise source) to place an isolator between the noise source and the receiver [12], in the proposed method, an isolator is not necessary, as the method implicitly reduces the error introduced by imperfect noise power transfer due to e.g. varying impedance mismatch between the on-state LNA and calibration switch. The cost associated with an isolator can, therefore, be avoided.

III. Results

As proof of concept, a 24-24.5 GHz modular downconversion WVR was used, featuring a nominal 6.5 dB NF and peak gain of 75 dB [13]. The ADL6010 envelope detector used for power detection features a non-negligible nonlinear response [14]. The antenna was emulated by a Mini-circuits ANNEF-50K+ 50 Ω 2.92 mm termination [15], of known physical temperature ($T_{P50\Omega}$), with the effective noise temperature equivalent to that of an observed scene of 50-100 K (the expected scene temperature from a potential mm-wave radio astronomy site) with 2.7 dB of antenna interconnect loss [2], [12], [16]. As a noise source, the CMD299K4 18-40 GHz LNA by Qorvo was utilized [17], terminated by another ANNEF-50K+ 50 Ω termination. Switching and bias control were automated using a BeagleBone Black single board computer as a controller, which also implemented the calibration algorithm. The V_{GG} bias voltage was kept constant at 3 V as recommended by the datasheet. The V_{DD} bias voltage was adjusted across n = 6 values (V_B = {0.7, 0.8, 0.9, 1.0, 1.5, 3} V), with corresponding initial T_N values of 700, 1200, 2000, 3400, 6700, 7400 K. $T_{N3.0V}$ was calculated using (2) and datasheet estimates of G and NF. The rest of the T_N values were chosen proportionally to V_N and a linear interpolation from $T_{N3.0V}$ and T_{N0}. No values where selected based on any measurements of the LNA.

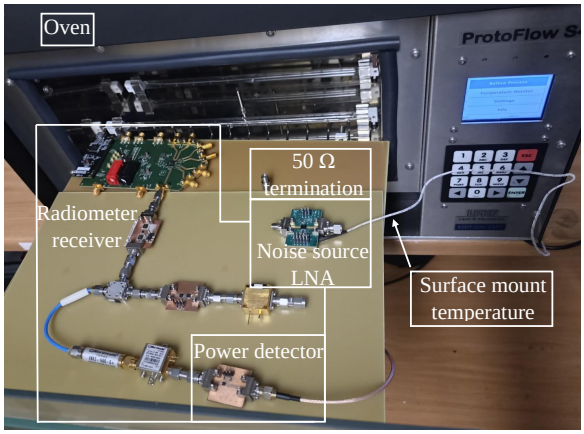

Fig. 2: Measurement setup with the WVR receiver, noise source LNA, power detector and 50 Ω load on the oven tray with the door open.

To simultaneously account for non-ideal noise power transfer between the output of the off-state LNA and the calibration switch, as well as from the antenna to the calibration switch, a one-time noise power measurement of a 50 Ω load at known physical temperature ($T_{P50\Omega}$) was performed, and the calibration procedure initiated to acquire the known T_{ANT} with d as variable. The error was minimized for a value of $d = 0.9$, which was subsequently used in calibration. While measurements of the complex port impedances of the switch, noise source and antenna could also be used to calculate [1], [16] separate correction terms for the antenna and the off-state LNA (d_{ANT} and $d_{LNA(off)}$), a single, average value proved sufficient for this application.

The radiometer and emulation load were placed in a laboratory oven (Figure 2), to induce both emulated scene temperature variation as well as variation in the response of the radiometer iteself. Measurements were taken at 5°C increments from 25°C to 75°C, with both emulated antenna and calibration load measuremetns taken at each increment.

This article has been accepted for publication in IEEE Microwave and Wireless Technology Letters. This is the author's version which has not been fully edited and content may change prior to final publication. Citation information: DOI 10.1109/LMWT.2024.3474971

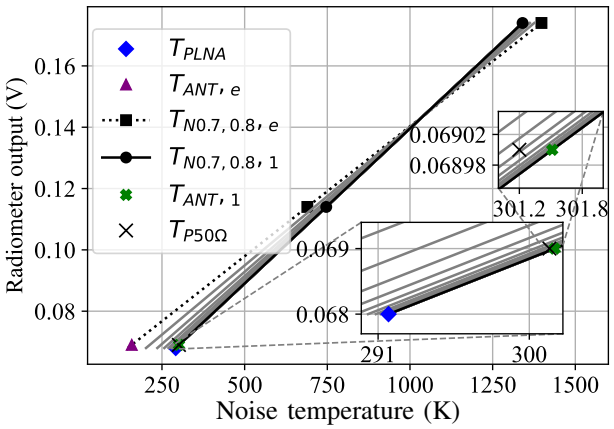

Fig. 3: $V_{N0.7V}$ and $V_{N0.8V}$ against estimated noise temperature with a fitted straight line for each iteration from the initial estimate (dotted line) to the final estimate (solid line) and iterations inbetween (grey lines).

Figure 3 shows the post-processing method using two points, $T_{N0.7V}$ and $T_{N0.8V}$. $T_{ANT,1}$ and $T_{ANT,e}$ is the estimates with and without post-processing respectively. The error between $T_{ANT,1}$ and $T_{P50\Omega}$ is 0.31 K.

Figure 4 shows this measured noise temperature with and without post-processing. While direct application of (1) results in error of over 800 K, the new post-processing method produced a mean error of 0.43 K and a maximum error of 1.23 K. This compares favourably with accuracies obtained with similar instruments in literature [18]–[20], and while it does not match that of temperature stabilized radiometers with <100 mK error [11], [21] used for VLBI correction, it meets the generally accepted benchmark of 0.5 K [22] for atmospheric monitoring, while presenting significant SWaP-C benefits. This demonstrates that the calibration procedure clearly accounts for the unknown calibration reference source using a thermocouple measurement as reference, and can produce an accurate calibration while presenting significant SWaP-C benefits. The calibration sequence typically required less than 500 ms to complete, which is negligible compared to the typical temporal resolution of the required measurements which is on the order of minutes [22], [23].

While the purpose of the proposed method is to estimate observed noise temperature, a one-time responsivity calibration of the power detector enables built-in Y-factor measurements to estimate the system's gain and NF. This was compared to an *in situ* DUT measurements using an Anritsu ME7828A VNA, as well as Y-factor measurement on a R&S FSW50 using a NW346V calibrated noise source and the K30 measurement option. Figure 5 shows the band-averaged DUT gain and NF using the different measurement techniques. Between the VNA measurement and the proposed method a mean gain measurement error of 0.68 dB was obtained, with a maximum error of 1.41 dB. Between the Y-factor measurement and the proposed method a mean NF error of 0.25 dB was obtained, with a maximum error of 0.55 dB.

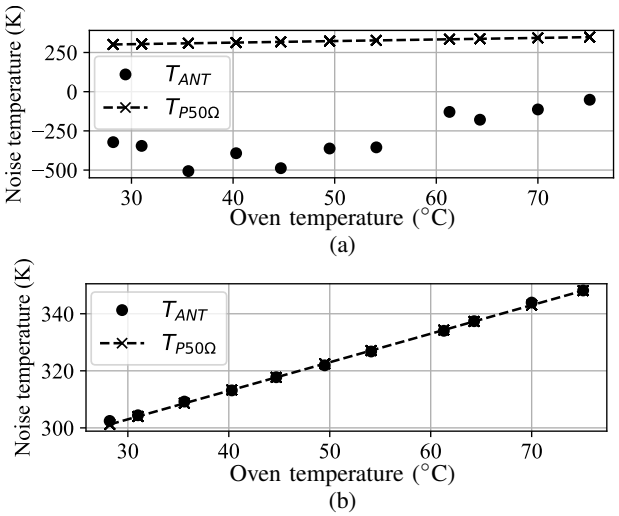

Fig. 4: Radiometric noise temperature (measured and estimated) over varying oven temperature (a) without post-processing, and (b) with post-processing.

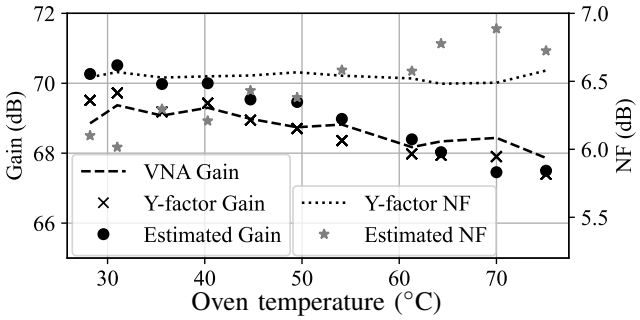

Fig. 5: Gain and NF measurements of the DUT.

IV. Conclusion

This study presents a novel calibration method for total power radiometers using an off-the-shelf low-noise amplifier (LNA) and source termination as the calibration source. The method does not require a calibrated noise source, and only approximate gain and noise figure (NF) data of the LNA. Experimental results show a mean error of 0.43 K compared to a block-body thermal measurement. When augmented with a one-time power detector calibration the method can be used with Y-factor calculations to predict system gain and NF. Future work will investigate the effect of reduced impedance mismatch in the noise chain by the inclusion of isolators or directional couplers, separate correction terms d_{ANT} and $d_{LNA(off)}$ (as well their temperature dependency), as well as a more rigorous analysis of the calibration method *in situ* with field trial data and comparison to other calibrated measurements and application to other types of radiometers.

Acknowledgements

The financial assistance of the South African Radio Astronomy Observatory (SARAO) towards this research is hereby acknowledged (www.sarao.ac.za).

REFERENCES

[1] F. T. Ulaby and D. K. Long, *Microwave Radar amd Radiometric Remote Sensing*. The University of Michigan Press, 2014.

[2] E. R. Westwater, S. Crewell, C. Mätzler, and D. Cimini, "Principles of Surface-based Microwave and Millimeter wave Radiometric Remote Sensing of the Troposphere," *Quad. Soc. Ital. Elettromagnetismo*, vol. 1, no. 3, pp. 50–90, 2005.

[3] D. Hiriart, P. Goldsmith, M. Skrutskie, and L. Salas, "Atmospheric Opacity at 215 GHz Over San Pedro Martir Sierra in Baja California," *Revista Mexicana de Astronomia y Astrofisica, 33, p. 59-68 (1997)*, vol. 33, pp. 59–68, 1997.

[4] T. Stander, R. Deane, D. I. de Villiers, A. de Witt, D. F. Rodríguez, D. Hiriart, S. E. Kurtz, F. van den Heever, and M. V. de la Rosa Becerra, "Progress toward improved water vapour radiometry: an overview of the South Africa-Mexico bilateral programme," *Ground-based and Airborne Telescopes VIII*, vol. 11445, pp. 270–278, 2020.

[5] D. Ferrusca, J. Cuazoson, J. Contreras, D. Hiriart, E. Ibarra, S. Kurtz, T. Stander, and M. Velázquez, "Embedded system upgrade based on Raspberry Pi computer for a 23/31 GHz dual-channel water vapor radiometer," in *Ground-based and Airborne Telescopes VIII*, vol. 11445. SPIE, 2020, pp. 1439–1448.

[6] G. Elgered and P. O. Jarlemark, "Ground-based microwave radiometry and long-term observations of atmospheric water vapor," *Radio Science*, vol. 33, no. 3, pp. 707–717, 1998.

[7] B. Burki, "Technical Documentation: WVRIII Microwave-Water-Vapor-Radiometer," ETH, Institute for Geodesy and Photogrammetry, Switzerland, Tech. Rep., 10 2000.

[8] L. Dunleavy, M. Smith, S. Lardizabal, A. Fejzuli, and R. Roeder, "Design and characterization of FET based cold/hot noise sources," in *1997 IEEE MTT-S International Microwave Symposium Digest*, vol. 3, 1997, pp. 1293–1296.

[9] L. Weijun, C. He, and X. Hao, "An Active Cold and Hot Noise Generator," in *2019 International Conference on Microwave and Millimeter Wave Technology (ICMMT)*, 2019, pp. 1–3.

[10] M. Leffel and R. Daniel, "Application Note: The Y Factor Technique for Noise Figure Measurements," Rohde & Schwarz, Tech. Rep., 10 2021.

[11] E. R. Westwater, S. Crewell, and C. Mätzler, "A Review of Surface-Based Microwave and Millimeter-Wave Radiometric Remote Sensing of the Troposphere," *URSI Radio Science Bulletin*, vol. 2004, no. 310, pp. 59–80, 2004.

[12] M. W. Pospieszalski, "On the Noise Parameters of Isolator and Receiver with Isolator at the Input," *IEEE Transactions on Microwave Theory and Techniques*, vol. 34, no. 4, pp. 451–453, 1986.

[13] R. Neate and T. Stander, "A Modular Water Vapour Radiometer for Comparing Water Vapour Radiometer Topologies and Calibration Techniques," *Ground-based and Airborne Telescopes X*, 2024.

[14] *Fast Responding, 45 dB Range, 0.5 GHz to 43.5 GHz Envelope Detector, ADL6010*, Analog devices, 2020.

[15] *Coaxial Termination, 50 Ω, DC to 40 GHz, 2.92 mm-Female, ANNEF-50K+*, Mini-Circuits, 2022.

[16] D. M. Pozar, *Microwave engineering*. John wiley & sons, 2011.

[17] *18-40 GHz Low Noise Amplifier, CMD299K4*, qorvo, 7 2021.

[18] G. Maschwitz, U. Löhnert, S. Crewell, T. Rose, and D. Turner, "Investigation of ground-based microwave radiometer calibration techniques at 530 hPa," *Atmospheric Measurement Techniques*, vol. 6, no. 10, pp. 2641–2658, 2013.

[19] F. Alimenti, S. Bonafoni, S. Leone, G. Tasselli, P. Basili, L. Roselli, and K. Solbach, "A Low-Cost Microwave Radiometer for the Detection of Fire in Forest Environments," *IEEE transactions on geoscience and remote sensing*, vol. 46, no. 9, pp. 2632–2643, 2008.

[20] M. Schneebeli and C. Matzler, "A Calibration Scheme for Microwave Radiometers Using Tipping Curves and Kalman Filtering," *IEEE transactions on geoscience and remote sensing*, vol. 47, no. 12, pp. 4201–4209, 2009.

[21] R. J. Sault, G. Carrad, P. Hall, and J. Crofts, "Radio path length correction using water vapour radiometry," *arXiv preprint astro-ph/0701016*, 2006.

[22] Y. Han and E. R. Westwater, "Analysis and Improvement of Tipping Calibration for Ground-Based Microwave Radiometers," *IEEE transactions on geoscience and remote sensing*, vol. 38, no. 3, pp. 1260–1276, 2000.

[23] A. B. Tanner and A. L. Riley, "Design and performance of a high-stability water vapor radiometer," *Radio Science*, vol. 38, no. 3, 2003.